

DIAGNOSTICS OF AND WITH LASER-INDUCED ENERGY MODULATION AT THE DELTA STORAGE RING*

S. Khan[†], S. Hilbrich, M. Höner, H. Huck, M. Huck,

C. Mai, A. Meyer auf der Heide, R. Molo, H. Rast, P. Ungelenk,

Center for Synchrotron Radiation (DELTA), TU Dortmund University, 44227 Dortmund, Germany

Abstract

DELTA is a 1.5-GeV synchrotron light source operated by the Center for Synchrotron Radiation at the TU Dortmund University. An interaction between electron bunches and femtosecond laser pulses is routinely used to generate ultrashort pulses of coherent synchrotron radiation at harmonics of the laser wavelength (coherent harmonic generation, CHG) as well as short and coherent pulses in the THz regime. The paper describes diagnostics methods to optimize the laser-electron overlap and to characterize the generated VUV and THz pulses. Furthermore, the laser-electron interaction can be employed as a beam diagnostics tool, e.g. to study the longitudinal steady-state bunch profile as well as dynamic properties during RF-phase modulation, which is applied to improve the beam lifetime.

INTRODUCTION

Synchrotron radiation (SR) sources based on electron storage rings [1] are complementary to high-gain free-electron lasers (FELs) [2] in various ways. The extreme peak brilliance of FELs has opened up new scientific opportunities, while the brilliance of SR sources, having increased by several orders of magnitude per decade, is still sufficient for many applications. Since high-gain FELs are based on linear accelerators, they serve only one experiment at a time with a relatively low pulse repetition rate, while SR sources are multi-user facilities producing very stable beams with a pulse rate of up to 500 MHz. The pulse duration of FELs is in the femtosecond regime allowing to study dynamic processes such as chemical reactions, structural and electronic changes in molecules or crystals, or fast magnetic phenomena, while the pulses from SR sources with a duration of 30 to 100 ps (FWHM) are inadequate for this purpose. Presently, four high-gain FELs are in user operation while about 50 SR sources exist worldwide. Reducing the pulse duration of SR sources by about three orders of magnitude would, therefore, increase the research opportunities for a very large user community.

While the electron bunches can be shortened to a few picoseconds by reducing the momentum compaction factor [3,4], sub-picosecond SR pulses are obtained by extracting radiation from a small longitudinal fraction (a "slice") of long electron bunches [5]. To this end, the electron energy is modulated by the electric field of a femtosecond laser pulse co-propagating with the bunch in an undulator. The

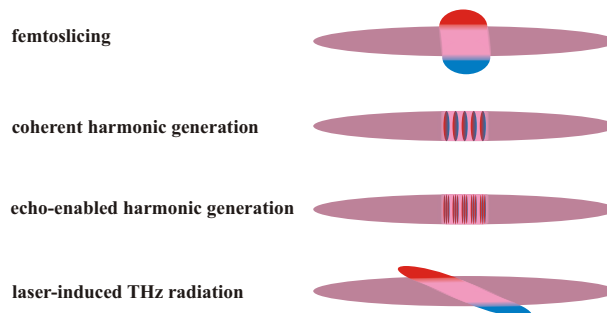


Figure 1: Laser-based methods to generate ultrashort SR pulses (see text). Note that the central "slice" of energy-modulated electrons (red and blue) is typically 1000 times shorter than the whole bunch.

modulation has the periodicity of the laser wavelength, an envelope similar to the laser pulse shape, and an amplitude proportional to the square root of the laser pulse energy. Typically, Ti:sapphire laser systems are employed with a wavelength of 800 nm, a pulse energy of a few mJ and a repetition rate in the kHz range, leading to a modulation amplitude of 5-10 times the rms energy spread within a slice of 1/1000 of the bunch length. An undulator used for this purpose is called "modulator". The laser-induced energy modulation may be employed in several ways (Fig. 1):

- Off-energy electrons are transversely displaced in magnets such that their short SR pulse from a second undulator (the "radiator") can be separated spatially from the long pulse produced by the other electrons. In this "femtosing" scheme [6], the radiator wavelength can be tuned to any value. Even though incoherent SR from a small fraction of the bunch is rather weak and the laser pulse rate is 10^{-5} of the bunch rate, this scheme produces significant scientific results at the ALS in Berkeley/USA [7,8], BESSY in Berlin/Germany [9,10], and the SLS in Villigen/Switzerland [11,12]. Another femtoslicing source is currently under commissioning at SOLEIL in Saint-Aubin/France [13].
- Using a dispersive chicane, the energy modulation may be translated into a periodic density modulation giving rise to coherent radiation at harmonics of the laser wavelength. Since the coherent SR intensity scales with the number of energy-modulated electrons squared [14], it is higher than the incoherent SR intensity from the rest of the bunch, and no spatial separation is required. This scheme, called CHG (coherent harmonic generation) [15], is restricted to harmonics $h < 10$ since

* Work supported by BMBF (05K13PEC), DFG (INST212/236-1), and by the state NRW.

[†] shaukat.khan@tu-dortmund.de

Table 1: Parameters of the DELTA Short-Pulse Facility

beam energy	1.5 GeV
circumference (revol. frequency)	115.2 m (2.6 MHz)
multibunch/single-bunch current	130/20 mA
horizontal emittance	15 nm rad
relative energy spread	0.0008
rms bunch length (duration)	13 mm (43 ps)
laser wavelength	800 nm
pulse energy at 800/400/267 nm	8.0/2.7/1.0 mJ
laser repetition rate	1 kHz
laser pulse duration	45 fs
undulator period length	250 mm
modulator/radiator periods	7/7
maximum undulator parameter K	12
maximum chicane strength R_{56}	130 μm

the coherent SR intensity decreases exponentially with increasing harmonic number. The CHG principle was demonstrated in the 1980s [16], and recent implementations were accomplished at Elettra near Trieste/Italy [17], UVSOR in Okazaki/Japan [18], and DELTA in Dortmund/Germany [19].

- A density modulation following a twofold laser-electron interaction has been proposed as an FEL seeding scheme but may as well be used to generate ultrashort pulses in storage rings. Known as EEHG (echo-enabled harmonic generation) [20], the advantage over CHG is that the coherent SR intensity follows $I_{\text{coh}} \sim h^{-2/3}$ and higher harmonics can be reached. EEHG has been demonstrated at two linac-based experiments at SLAC in Menlo Park/USA [21] and SINAP in Shanghai/China [22], and has been proposed for the storage rings SOLEIL [23] and DELTA [24].
- Due to the energy-dependent path lengths along the storage-ring lattice, the energy-modulated electrons leave a short dip in the longitudinal charge density giving rise to coherent radiation pulses in the terahertz (THz) regime over several turns, see e.g. [25]. These short and intense pulses are used at several facilities (ALS, BESSY, SLS, UVSOR, DELTA) as energy-modulation diagnostics, but can also be employed for time-resolved far-infrared spectroscopy.

In the following, techniques used at the CHG facility at DELTA to diagnose and optimize the laser-electron interaction are described. Most of these methods are relevant to other short-pulse sources (CHG, EEHG, or femtoslicing) and to seeded FELs. In addition, laser-induced energy modulation can be used as a beam diagnostics tool, e.g. to sample the longitudinal charge distribution. Interacting only with 1/1000 of the electrons, the effect on the bunch is small but not always negligible. The energy modulation can, for example, trigger an instability leading to coherent THz bursts [26].

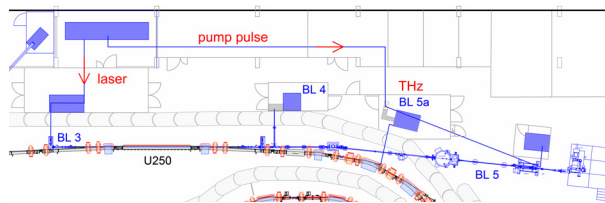


Figure 2: Short-pulse facility at DELTA comprising a laser system, the beamline BL 3 sending seed pulses to the undulator U250, the diagnostics beamline BL 4, the VUV beamline BL 5 and the THz beamline BL 5a.

THE SHORT-PULSE FACILITY AT DELTA

DELTA is a 1.5-GeV synchrotron light source operated by the Center for Synchrotron Radiation at the TU Dortmund University. A facility to generate ultrashort and coherent SR pulses in the VUV and THz regime was constructed in 2011 [19, 24]. Its footprint is shown in Fig. 2, relevant parameters are given in Tab. 1. Pulses from a femtosecond Ti:sapphire laser system or a harmonic thereof modulate the electron energy in the first 7 periods of the electromagnetic undulator U250 tuned to the seed wavelength, while 3 further periods are powered to form a dispersive chicane. The last 7 periods are tuned to a harmonic of the seed wavelength and act as radiator sending coherent pulses either via beamline BL 4 to a diagnostics hutch or to the experiment at BL 5. This beamline, operated by the Forschungszentrum Jülich, comprises a plane-grating monochromator and a photoelectron spectrometer with a 2-dimensional detector for spectral and angular sensitivity. In addition, a dedicated THz beamline (BL 5a) was constructed, which is equipped with an InSb bolometer, a fast $\text{YBa}_2\text{Cu}_3\text{O}_{7-x}$ (YBCO) detector, and an FT-IR spectrometer using a Si bolometer as detector. An evacuated beam pipe allows to send laser pulses directly to BL 5 and BL 5a for pump-probe applications.

In the past, the undulator U250 was operated as a storage-ring FEL in optical-klystron configuration, lasing in the visible regime at reduced beam energies around 0.5 GeV [27]. New power supplies allow to tune the modulator to a seed wavelength of 800 nm at the nominal beam energy of 1.5 GeV, making CHG during user operation possible. Accelerator physics studies can be performed during 10 weeks/year and, in addition, in a shift following the Mo-Fr user operation at 20 weeks/year. During machine studies, CHG is predominantly performed in single-bunch mode with a current of up to 20 mA and a seed wavelength of 800 or 400 nm. In user operation, CHG was demonstrated using a hybrid fill pattern (120 mA multibunch plus a 10-mA single bunch). The final goal is seeding with 267 nm and generating ultrashort pulses at 53 nm for pump-probe experiments. As an upgrade, the 6 m long straight section of the U250 will be extended to 20 m by rearranging the dipole magnets in order to accommodate two new electromagnetic modulators (7 periods, period length 200 mm, to be delivered by the end of 2014) and the U250 as radiator for EEHG [28].

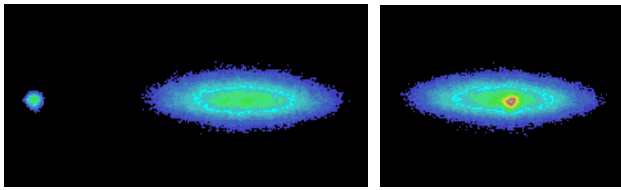


Figure 3: Streak camera images of a femtosecond laser pulse preceding the undulator radiation by 200 ps (left) and of overlapping pulses (right). The apparent laser pulse duration is given by the camera resolution.

THE LASER-ELECTRON OVERLAP

For optimum energy modulation, a number of conditions must be met:

- The undulator spectrum must overlap with the laser spectrum, which is not critical due to the large undulator bandwidth. The electric field vector of the laser must be parallel to the electron motion in the planar undulator.
- The laser arrival time should be that of the bunch center. To this end, the laser oscillator is synchronized to the radio frequency (RF) of the storage ring by piezo-tuning the laser cavity, and the 1-kHz laser amplifier timing is set for the desired RF bucket by a revolution trigger which is vetoed for 1 ms. The laser timing was initially fine-tuned by delaying the RF signal using a mechanical phase shifter ("trombone"), but now a vector modulator is employed. The arrival time of SR from the modulator and the (strongly attenuated) laser pulse is measured using a fast photodiode and a streak camera (Fig. 3).
- The energy modulation depends critically on the spatial overlap of laser and electron bunch at the center of the modulator, but is less sensitive to angular errors. In the evacuated seed beamline BL 3, good control over position and angle is achieved by two mirrors with reproducible and backlash-free angular tunability (M1 and M2 in Fig. 4). Since the beam cannot be intercepted

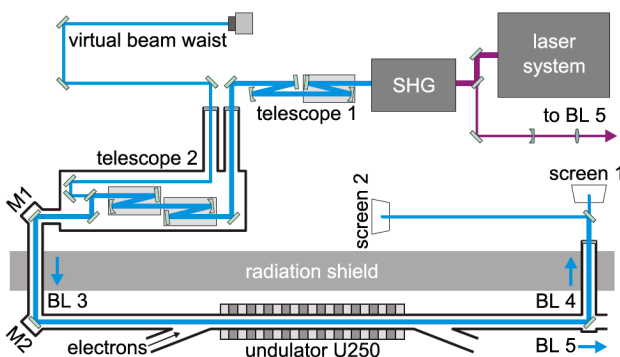


Figure 4: Laser beam path at DELTA with two mirror telescopes (currently under construction). Telescope 1 (in air) enlarges the laser beam, telescope 2 (in vacuum) provides the final focusing.

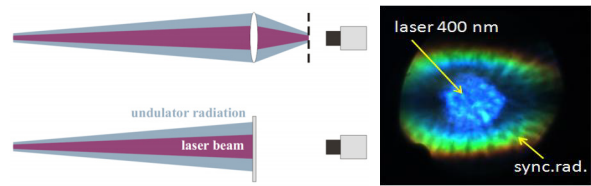


Figure 5: Two methods to image undulator and laser light with (top) or without (bottom) focusing. A typical screen image without focusing (right) shows the frequency-doubled laser as a blue spot surrounded by undulator radiation.

by screens in a storage ring, the transverse overlap is not easy to judge. Laser light and SR from the modulator is viewed on a screen without focusing (obtaining the overlap at the screen position) or, alternatively, using cameras equipped with lenses (obtaining the overlap at the focal point), see Fig. 5. Splitting the beam and using two screens at different positions or two different focal points, respectively, allows to obtain spatial and angular information (screen 1 and 2 in Fig. 4). In either case, the optical quality suffers from aperture limitations and from deformations or radiation damage of the light-extracting mirror.

- The optimum laser waist position is usually at the modulator center. For an on-axis electron, the maximum energy change is obtained if the Rayleigh length is about $1/4$ of the modulator length [29]. The finite electron beam size and a laser quality factor $M^2 > 1$, however, requires to increase the Rayleigh length $z_R = \pi w_0^2 / \lambda$ and thus the $1/e^2$ laser waist radius w_0 in order to obtain a sufficient modulation averaged over all electrons. The waist size and position is controlled by changing the positions of focusing lenses or mirrors, usually associated with transverse "steering" of the laser beam. After focusing, leakage through a dielectric mirror is picked off and sent to a point at an equal distance as the modulator. This "virtual laser waist" is inspected by a CCD camera movable on a rail (Fig. 4).
- The laser pulse quality at the modulator is critical. It suffers from spherical aberrations and astigmatism from mirrors and lenses. The transition through lenses, vacuum windows, and even air causes focusing due to the intensity-dependent index of refraction ("*B* integral"), chirp due to group-delay dispersion, and chromatic aberrations. The wavefronts may be distorted by air turbulence and thermal effects in glass. In the configuration shown in Fig. 5, the first telescope in air enlarges the laser beam to reduce the power density on the vacuum window, while the second telescope in vacuum provides the final focusing.

The occurrence of coherent THz radiation detected by the InSb bolometer at beamline BL 5a is a very sensitive indicator of successful energy modulation [25], another one is the CHG signal.

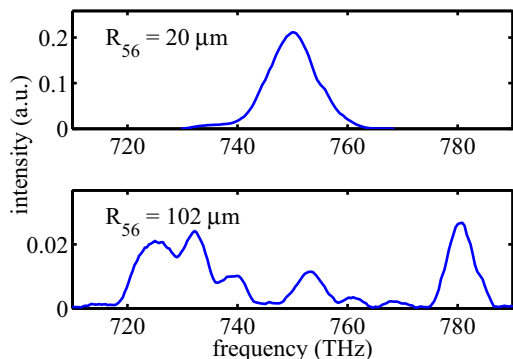


Figure 6: CHG spectra at 400 nm (frequency 750 THz) with the chicane set for optimum density modulation (top) and with a larger R_{56} value (bottom).

The energy-modulation amplitude ΔE_{\max} can be measured by observing the beam lifetime while reducing the energy acceptance of the storage ring. This can be done using a scraper in combination with dispersion [9] or by reducing the RF voltage. In the case of CHG, optimum bunching is obtained at a constant value of $R_{56} \cdot \Delta E_{\max} / \sigma_E$, from which the modulation amplitude can be deduced. Here, σ_E is the energy spread and the chicane strength R_{56} , if uncertain, can be obtained from the fringe pattern of an optical-klystron spectrum, see e.g. [30].

CHARACTERIZATION OF RADIATION

A general issue when detecting CHG radiation is how to reject the strong co-propagating seed pulses. When seeding at a wavelength of 800 nm, CHG radiation at 400 nm passes a dielectric mirror coated for the seed wavelength. To study CHG pulses at shorter wavelengths, which would not pass a mirror substrate, several dielectric mirrors deflecting CHG radiation while transmitting the seed pulses are used in combination with bandpass filters.

The spectrum of spontaneously emitted (SE) undulator radiation and CHG pulses is measured using a Czerny-Turner-type monochromator followed by an avalanche photodiode (APD). For a selected wavelength, a digital oscilloscope records the CHG+SE intensity as well as the SE intensity at the following revolution without laser-electron interaction, observing a CHG-to-SE ratio of up to 10^3 . The spectra obtained this way match those obtained by scanning the plane-grating monochromator in beamline BL 5 while recording the photoelectron yield or by using a CCD-line spectrometer [24]. In the latter case, the CCD records the whole spectrum at once but integrates over 2600 SE pulses for each CHG pulse. For the case of low harmonics, however, the strong CHG component is nevertheless visible. The SE spectrum has a width of $\Delta\nu/\nu \approx 1/N$ (FWMH), where $N = 7$ is the number of radiator periods, and shows fringes from the interference between the radiator and the corresponding harmonic of the modulator [30]. The CHG spectrum is narrower with a time-bandwidth product close to the Fourier limit,

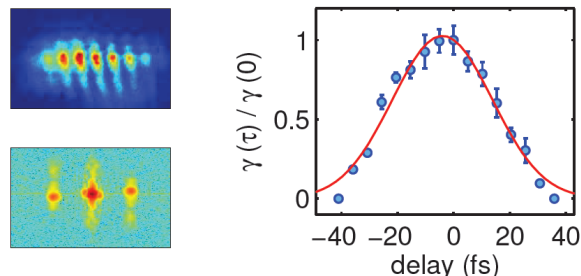


Figure 7: Double-slit pattern of 200-nm CHG radiation in real (left, top) and spatial frequency space (left, bottom), and dependence of the fringe visibility on the delay τ between light from the two slits. Here, $\gamma(\tau)$ is the ratio of the integrated intensities of a sideband and the central peak in frequency space.

provided that the R_{56} transfer matrix element of the chicane is tuned for optimum density modulation (Fig. 6, top). As an example, a width of 2.6 nm (FWHM) was measured at BL 5 for 200-nm CHG radiation. Increasing the chicane strength leads to a broader CHG spectrum with interference fringes (Fig. 6, bottom), which can be explained by a more complex density modulation. The energy modulation follows the Gaussian shape of the laser pulse, and its maximum is overbunched, i.e. the optimum value of $R_{56} \cdot \Delta E_{\max} / \sigma_E$ is exceeded, if R_{56} is too large (see [32]).

The CHG pulse energy can be estimated from the observed CHG-to-SE ratio and the SE intensity measured with a powermeter. As an example, a pulse energy of 0.2 nJ was obtained at 200 nm (the 4th harmonic of 800 nm), corresponding to $2 \cdot 10^8$ photons per pulse [31]. The angular distribution of CHG and SE at a selected wavelength is obtained by scanning the radiation over the spectrometer entrance slit. In accordance with the respective spectral widths, the angular distribution of CHG is narrower than that of SE.

For radiation emitted by micro-bunched electrons, which is the case for FEL as well as CHG radiation, the coherence properties are of particular interest. In all coherence measurements, a fast-gated intensified CCD camera is essential in order to obtain sufficient single-shot intensity from a single turn without adding SE pulses [33]. The transverse coherence is studied using a classical double-slit setup followed by the camera after 1.3 m [32]. The visibility of interference fringes reduces with increasing slit separation, and the separation with 50% reduction defines the transverse coherence length. Here, the visibility $V = (I_{\max} - I_{\min}) / (I_{\max} + I_{\min})$ can either be obtained by directly observing the maximum and minimum intensity in forward direction or by performing a 2-dimensional Fourier transform (Fig. 7, left). In spatial frequency space, the fringes appear as sidebands adjacent to a central peak, and their integral intensity is proportional to V [34]. A typical transverse coherence length of 1 mm is obtained at a distance of 10 m from the radiator.

The longitudinal coherence can be estimated from the off-axis fringe visibility in the double-slit pattern, but more accurate results are obtained from dedicated experiments.

In one measurement, the length of one arm of a Michelson interferometer was varied while recording the interference pattern. Another experiment employed the double-slit setup with movable glass wedges to delay the light from one slit with respect to the other (Fig. 7, right). In either case, the longitudinal coherence length is derived from the dependence of the fringe visibility on the delay. In reasonable accordance with the measured spectral widths, a coherence length of 34 fs was obtained with both methods for CHG and 10 fs for SE [31, 32], where the SE spectrum was narrowed by a bandpass filter. Yet another approach to study the coherence is to record speckle patterns [35] of CHG pulses passing through a diffuse organic film. After successful application at FELs, e.g. [36], speckle measurements were performed at DELTA and are currently under analysis [37].

LONGITUDINAL BEAM DIAGNOSTICS

The longitudinal electron density distribution $\rho(t - t_0)$ can be sampled by moving the laser arrival time t relative to that of the bunch center (t_0) and recording either the CHG or coherent THz signal, both being proportional to ρ^2 . The bunch length obtained this way is ≈ 100 ps (FWHM), in accordance with streak camera measurements [38]. The longitudinal fine structure imprinted on the bunch, i.e. the aforementioned "dip" which gives rise to coherent THz radiation, can be studied in the frequency domain by measuring the THz spectrum, and the results obtained at DELTA agree well with a model calculation [39]. Direct measurements in the time domain were not yet performed but can be done with sub-ps resolution by electro-optical sampling either in the far field [40] or in the near field [41].

The laser-induced energy modulation was also used to study dynamic changes of the bunch shape. A periodic modulation of the RF phase by twice the synchrotron frequency is routinely applied at DELTA to suppress longitudinal instabilities and to improve the beam lifetime [42]. Depending on the modulation amplitude, the bunch length changes periodically or the electrons populate two or even three "islands" rotating about each other in longitudinal phase space [43, 44]. Two methods were applied to perform CHG while the RF-phase modulation was in operation [45]:

(a) The modulation frequency f_m was tuned close to an integer multiple (e.g. $n = 32$) of the laser repetition rate f_l such that the laser-electron interaction takes place at a slowly changing phase of the RF modulation. The CHG and THz signal oscillate on a typical time scale of a minute (Fig. 8), depending on the frequency difference $f_m - n \cdot f_l$.

(b) The modulation frequency was synchronized to the laser pulses by using a trigger at a rate of f_l to start a train of modulation cycles, and at the end of an integer number of cycles, the trigger starts the next train. In this case, a delay applied to the trigger selects a constant modulation phase at which the laser-electron interaction takes place.

Depending on f_m and the modulation amplitude, the beating behavior of the CHG and THz signal in method (a) can be in phase or 180° out of phase, as shown in Fig. 8. If the

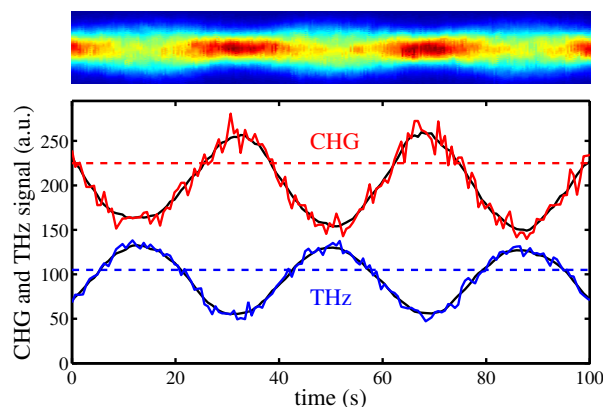


Figure 8: Streak camera image (top) and CHG/THz signal intensities versus time (bottom) in the presence of an RF-phase modulation (see text for details). The dashed lines indicate the respective steady-state values without modulation.

modulation is weak, the bunch length and energy spread oscillate in a countercyclical way. The CHG signal follows the electron density at the bunch center while the THz signal measured by the InSb bolometer decreases strongly with increasing energy spread. This assumption is confirmed when the laser arrival time is tuned away from the bunch center at which the electron density is larger when the bunch is shorter. If the laser pulse is delayed as to intercept the bunch tail, the interacting electron density is larger when the bunch is longer, and the CHG and THz signals are in phase.

While method (a) is convenient to study the full period of the RF phase modulation, method (b) is the one to be employed for CHG in user operation. In both cases, a CHG signal up to 30% larger than without modulation was observed suggesting that the bunch is temporarily shorter than its equilibrium length.

OUTLOOK

With several femtoslicing and CHG facilities in operation and the advent of seeded high-gain FELs [46], the laser-based manipulation and diagnostics of relativistic electron beams [47] has become a standard method, although achieving and maintaining an optimum laser-electron overlap is still a laborious task. Newly emerging schemes like EEHG [20] and other recently proposed ideas, e.g. phase merging [48], suggest that there is still room for improvement. Once this technology has matured, it may be possible to explicitly design a storage ring as a "pump-probe factory" with multiple laser-based short-pulse beamlines dedicated to ultrafast science.

ACKNOWLEDGEMENTS

It is a pleasure to thank our colleagues at DELTA and other institutes, particularly FZJ in Jülich, HZB in Berlin, DESY in Hamburg and KIT in Karlsruhe, for their continuous support and advice.

REFERENCES

- [1] Z.T. Zhao, "Storage Ring Light Sources", in *Reviews of Accelerator Science and Technology*, Vol. 3, edited by A. W. Chao and W. Chou, ISBN: 978-981-434038-0, World Scientific (2010), p. 57.
- [2] P. Schmüser, M. Dohlus, J. Rossbach, S. Behrens, *Ultra-violet and Soft X-Ray Free-Electron Lasers*, ISBN: 978-3-31904080-6, Springer (2014).
- [3] M. Abo-Bakr et al., "Brilliant, Coherent Far-Infrared (THz) Synchrotron Radiation", *Phys. Rev. Lett.* 90, 094801 (2003).
- [4] A.-S. Müller et al., "Far-Infrared Coherent Synchrotron Edge Radiation at ANKA", *Sync. Rad. News* 19(3), 18 (2006).
- [5] A. Zholents, "Electron-Beam-Based Sources of Ultrashort X-ray Pulses", in *Reviews of Accelerator Science and Technology*, Vol. 3, edited by A. W. Chao and W. Chou, ISBN: 978-981-434038-0, World Scientific (2010), p. 237.
- [6] A. A. Zholents, M. S. Zolotarev, "Femtosecond X-Ray Pulses of Synchrotron Radiation", *Phys. Rev. Lett.* 76, 912 (1996).
- [7] R.W. Schoenlein et al., "Generation of Femtosecond Pulses of Synchrotron Radiation", *Science* 287, 2237 (2000).
- [8] A. Cavalleri et al., "Band-Selective Measurements of Electron Dynamics in VO₂ Using Femtosecond Near-Edge X-Ray Absorption", *Phys. Rev. Lett.* 95, 067405 (2005).
- [9] S. Khan et al., "Femtosecond Undulator Radiation from Sliced Electron Bunches" *Phys. Rev. Lett.* 97, 074801 (2006).
- [10] I Radu et al., "Transient Ferromagnetic-like State Mediating Ultrafast Reversal of Antiferromagnetically Coupled Spins", *Nature* 472, 205 (2011).
- [11] P. Beaud et al., "Spatiotemporal Stability of a Femtosecond Hard-X-Ray Undulator Source Studied by Control of Coherent Optical Phonons", *Phys. Rev. Lett.* 99, 174801 (2007).
- [12] S.L. Johnson et al., "Direct Observation of Non-fully-symmetric Coherent Optical Phonons by Femtosecond X-ray Diffraction", *Phys. Rev. B* 87, 054301 (2013).
- [13] P. Prigent et al., "Progress on the Femto-Slicing Project at the Synchrotron SOLEIL", *J. Phys.: Conf. Series* 425, 072022 (2013).
- [14] H. Wiedemann, "Particle Accelerator Physics", ISBN: 978-3-54049043-2, Springer (2007).
- [15] R. Coisson, F.D. Martini, "Free-Electron Relativistic Scatterer for UV-Generation", in *Physics of Quantum Electronics: Free-Electron Generators of Coherent Radiation*, Vol. 9, edited by S. F. Jacobs et al., ISBN: 978-0-20105689-1, Addison-Wesley (1982), p. 939.
- [16] B. Girard et al., "Optical Frequency Multiplication by an Optical Klystron", *Phys. Rev. Lett.* 53, 2405 (1984).
- [17] E. Allaria et al., "Experimental Characterization of Nonlinear Harmonic Generation in Planar and Helical Undulators", *Phys. Rev. Lett.* 100, 174801 (2008).
- [18] M. Labat et al., "Optimization of a Seeded Free-Electron Laser with Helical Undulators", *Phys. Rev. Lett.* 101, 164803 (2008).
- [19] S. Khan et al., "Coherent Harmonic Generation at DELTA: A New Facility for Ultrashort Pulses in the VUV and THz Regime" *Sync. Rad. News* 24(5), 18 (2011).
- [20] G. Stupakov, "Using the Beam-Echo Effect for Generation of Short-Wavelength Radiation", *Phys. Rev. Lett.* 102, 074801 (2009).
- [21] D. Xiang et al., "Demonstration of the Echo-Enabled Harmonic Generation Technique for Short-Wavelength Seeded Free Electron Lasers", *Phys. Rev. Lett.* 105, 114801 (2010).
- [22] Z.T. Zhao et al., "First Lasing of an Echo-Enabled Harmonic Generation Free-Electron Laser", *Nature Photonics* 6, 360 (2012).
- [23] C. Evain et al., "Soft X-ray Femtosecond Coherent Undulator Radiation in a Storage Ring", *New. J. of Phys.* 14, 023003 (2012).
- [24] S. Khan et al., "Generation of Ultrashort and Coherent Synchrotron Radiation Pulses at DELTA" *Sync. Rad. News* 26(3), 25 (2013).
- [25] K. Holldack et al., "Femtosecond Terahertz Radiation from Femtoslicing at BESSY", *Phys. Rev. Lett.* 96, 054801 (2006).
- [26] J.M. Byrd et al., "Laser Seeding of the Storage-Ring Microbunching Instability for High-Power Coherent Terahertz Radiation", *Phys. Rev. Lett.* 97, 074802 (2006).
- [27] D. Nölle et al. "First lasing of the FELICITA I FEL at DELTA", *Nucl. Inst. Methods A* 445, 128 (2000).
- [28] S. Hilbrich et al., "Upgrade Plans for the Short-pulse Facility at DELTA", *Proc. of the Free Electron Laser Conference 2014, Basel, Switzerland, MPO087*, <http://jacow.org/>.
- [29] A.A. Amir, Y. Greenzweig, "Three-dimensional Theory of the Free-Electron Laser", *Phys. Rev. A* 34, 4809 (1986).
- [30] D.A.G. Deacon et al., "Optical Klystron Experiments for the ACO Storage Ring Free Electron Laser", *App. Phys. B* 34, 207 (1984).
- [31] M. Huck, dissertation, TU Dortmund University (in preparation).
- [32] M. Huck et al., "Ultrashort and Coherent Radiation for Pump-probe Experiments at the DELTA Storage Ring", *Proc. of the International Particle Accelerator Conference 2014, Dresden, Germany, 1848*.
- [33] A fast-gated iCCD camera was generously provided by B. Schmidt and S. Wunderlich (DESY Hamburg).
- [34] A. Singer et al., "Spatial and Temporal Coherence Properties of Single Free-Electron Laser pulses", *Opt. Express* 20, 17480 (2012).
- [35] J.W. Goodman, *Speckle Phenomena in Optics* ISBN: 978-1-93622114-1, Roberts & Company (2010).
- [36] S. Lee et al., "Single-shot Speckle and Coherence Analysis of the Hard X-ray Free Electron Laser LCLS", *Opt. Express* 21, 24647 (2013).
- [37] C. Gutt et al., "Femtosecond Speckle and Coherence Experiments at the CHG Short-Pulse Facility DELTA", *International Workshop on Phase Retrieval and Coherent Scattering, Evanston, USA (2014)*, P8.
- [38] P. Ungelenk et al., "Recent Developments at the DELTA THz Beamline", *Proc. of the International Particle Accelerator Conference 2012, New Orleans, USA, 768*.
- [39] P. Ungelenk et al., "Temporal and Spectral Observation of Laser-induced THz Radiation at DELTA", *Proc. of the International Particle Accelerator Conference 2013, Shanghai, China, 94*.

- [40] F. Müller et al., "Electro-optical measurement of sub-ps structures in low-charge electron bunches", *Phys. Rev. ST - Accel. Beams* 15, 070701 (2012).
- [41] N. Hiller et al., "Status of Single-shot EOSD Measurement at ANKA", *Proc. of the International Particle Accelerator Conference 2014, Dresden, Germany, 1909*.
- [42] S. Khan, J. Fürsch, P. Hartmann, T. Weis, "Studies and Control of Coupled-bunch Instabilities at DELTA", *Proc. of the International Particle Accelerator Conference 2010, Kyoto, Japan, 2755*.
- [43] H. Huang et al., "Experimental Determination of the Hamiltonian for Synchrotron Motion with RF Phase Modulation", *Phys. Rev. E* 48, 4678 (1993).
- [44] J. Byrd, W.-H. Chen, F. Zimmermann, "Nonlinear Effects of Phase Modulation in an Electron Storage Ring", *Phys. Rev. E* 57, 4706 (1998).
- [45] A. Meyer auf der Heide et al., "Coherent Harmonic Generation at the DELTA Storage Ring: Towards User Operation", *Proc. of the Free Electron Laser Conference 2014, Basel, Switzerland, TUP082*.
- [46] E. Allaria et al., "Highly coherent and stable pulses from the FERMI seeded free-electron laser in the extreme ultraviolet", *Nature Photonics* 6, 669 (2012).
- [47] E. Hemsing, G. Stupakov, D. Xiang, A. Zholents "Beam by Design: Laser Manipulation of Electrons in Modern Accelerators", *Rev. Mod. Phys.* 86, 897 (2014).
- [48] H. Deng, C. Feng, "Using Off-Resonance Laser Modulation for Beam-Energy-Spread Cooling in Generation of Short-Wavelength Radiation", *Phys. Rev. Lett.* 111, 084801 (2013).